AIAA JOURNAL
Vol. 31, No. 2, February 1993

Layer-Wise Approach for the Bifurcation Problem in Laminated Composites with Delaminations

Jaehong Lee,* Zafer Gürdal,† and O. Hayden Griffin Jr.†
Virginia Polytechnic Institute and State University, Blacksburg, Virginia 24061

Buckling of axially loaded composite beam plates with multiple delaminations is studied. The delaminations are assumed to extend through the width of the composite. A finite element method based on a layer-wise plate theory is developed to formulate the problem. Numerical results are obtained, addressing the effects of the number of delaminations, their lengths, through-the-thickness locations, and axial locations on the critical buckling load and corresponding mode shapes of the composite laminate. It is found that the proposed approach is very efficient and yields accurate solutions with significant savings in computing time compared with the commonly used plane elasticity finite element method for analyzing delamination buckling problems in composites.

Nomenclature

$A_{11}, B_{11}^i, D_{11}^{ij}, E_{11}^i, F_{11}^{ij}$	= in-plane laminate stiffnesses
$A_{55}, B_{55}^i, D_{55}^{ij}, E_{55}^i, F_{55}^{ij}$	= transverse laminate stiffnesses
a	= half-length of delamination
E_1, E_2	= Young's moduli along longitudinal and transverse fiber directions
e	= distance from support to center of delamination
G_{12}	= in-plane shear modulus of lamina
h	= half-thickness of beam
$l(=L/2)$	= half-length of beam
$N_x, N_x^j, \tilde{N}_x^i$	= in-plane stress resultants
$N_x^o, N_x^{jo}, \tilde{N}_x^{ijo}$	= in-plane compressive loads
n, n^j, n^{ij}	= specified values of in-plane forces
$Q_x, Q_x^j, \tilde{Q}_x^i$	= transverse shear-stress resultants
$\bar{Q}_{11}^{(k)}, \bar{Q}_{55}^{(k)}$	= transformed lamina stiffness matrices
t	= thickness of sublaminate
U	= strain energy
u, w	= displacements in x and z directions at reference surface
u^j	= nodal values of displacements in x direction of each lamina
$\bar{u}^i, \bar{w}^i$	= jumps in the slipping and opening displacements, respectively
V	= potential energy due to in-plane loads
Π	= total potential energy
$[K]$	= stiffness matrix
$[S]$	= geometric stiffness matrix
$\{\Delta\}$	= eigenvector of nodal displacements
λ	= eigenvalue
ν_{12}	= Poisson's ratio
ϵ_x, γ_{xy}	= normal and shear strains
σ_x, τ_{xy}	= normal and shear stresses
$\phi^j(z)$	= Lagrangian interpolation function
$\delta^i(z)$	= unit step function

Received March 13, 1992; presented as Paper 92-2224 at the AIAA/ASME/ASCE/AHS/ASC 33rd Structures, Structural Dynamics, and Materials Conference, Dallas, TX, April 13-15, 1992; revision received July 3, 1992; accepted for publication July 27, 1992.

*Research Associate, Department of Engineering Science and Mechanics. Member AIAA.

†Associate Professor, Department of Engineering Science and Mechanics. Senior Member AIAA.

Introduction

DELAMINATION is a commonly observed damage mode in composite laminates. Delamination may develop as a result of manufacturing defects or as a result of certain in-service factors, such as low-velocity impact by foreign objects. Delamination damage is known to cause degradation of overall stiffness and strength. In particular, delamination damage can result in substantial loss of compressive load carrying capacity of a laminate through local instability in the vicinity of a delamination, and can lead to global structural failure at loads well below the design level for an undamaged laminate.

With the increasing use of composites, compression behavior of delaminated composites has received considerable attention in recent years. Several authors have investigated various aspects of buckling and postbuckling behavior of delaminated structures. Chai et al.[1] may have been the first investigators to study this problem. They presented a one-dimensional analytical model to assess the compressive strength of a delaminated composite. Simitses and his collaborators[2-4] investigated delamination buckling and growth of simply supported and clamped composite plates using one-dimensional beam-plate theory. The effects of delamination position, length, and laminate thickness on buckling loads were studied. The problem of symmetric local buckling and growth of a delamination in a circular plate was presented by Bottega and Maewal.[5] Sheinman et al.[6] extended the work of Simitses et al.[2] to include the effect of bending-extension coupling on the stability of a delaminated composite using a finite difference model. Kardomateas and Schmueser[7] studied the effects of transverse shearing on buckling and postbuckling of delaminated composites. They found that these shear effects increase the possibility of crack growth due to the extra energy from the transverse forces. More recently, Chen[8] investigated transverse shear effects using variational energy principles. Results of Chen's study showed that the transverse shear effect depends on delamination location and size.

Most of the literature cited above employed analytical models for solution of the problem by dividing the delaminated beam into four regions (Fig. 1), and then applying boundary conditions for the outside edges and continuity conditions along the interfaces of the regions. Boundary conditions were

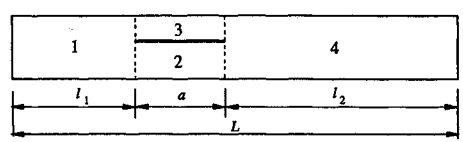

Fig. 1 Conventional one-dimensional delamination model.

generally assumed to be simply supported or clamped. For more general boundary conditions and multiple delaminations, finite element analysis is often employed. For example, a plane-elasticity finite element model was applied by Whitcomb,[9] Wang et al.,[10,11] and Williams et al.[12] to study delamination buckling and postbuckling in composites. However, analyses based on two-dimensional finite element models are computationally intensive because of the need for a very fine mesh near the delamination crack tip. Kapania and Wolfe[13] developed a one-dimensional finite element model based on the model suggested by Simitses et al.[2] to study the effect of multiple delaminations. However, their analysis was limited to two delaminations, and more general configurations were not studied.

To the authors' knowledge, most of the literature on delamination buckling of composite laminates deals with a single delamination, with only a few references[10,11,14,15] on multiple delamination problems. In actual situations, however, when composite laminates are subjected to impact, a number of delaminations with a complicated through-the-thickness distribution may occur. Therefore, there is need for an analytical capability that can be applied to general multiple delaminations with complex geometry. Most recently, Barbero and Reddy[16] adopted layer-wise plate theory,[17] which is capable of modeling multiple delaminations, to calculate strain-energy release rate. However, all of the examples considered in that work were limited to single near-the-surface delamination cases.

In the present study, a displacement-based, one-dimensional finite element model based on the layer-wise plate theory of Reddy[17] is developed to predict critical loads and corresponding buckling modes for a multiply delaminated composite with arbitrary boundary conditions. Governing equations are derived from the principle of the stationary value of total potential energy. It is assumed that through-the-width delaminations of prescribed distribution existed before loading is applied and that propagation of the delamination is ignored. Such an assumption is valid for tough materials where delamination propagation is not likely. Results are obtained for specially orthotropic laminates axially loaded between two clamped edges, and are compared with the results of Chen[8] and Wang et al.[10,11] for verification. For general multiple delamination configurations, the effects of one to seven delaminations with various locations, lengths, and shapes on critical buckling load and buckling mode are parametrically studied.

Formulation

Kinematics

An N-layer fiber-reinforced composite beam plate containing multiple through-the-width delaminations is considered (Fig. 2). To model the multiple delamination, the assumed displacement field is supplemented with unit step functions which allow discontinuities in the displacements as suggested by Barbero and Reddy.[16] The resulting in-plane and out-of-plane displacements, u_1 and u_3, at a generic point x, z in the laminate are assumed to be of the form

$$u_1(x, z) = u(x) + \sum_{j=1}^{N} \phi^j(z) u^j(x) + \sum_{i=1}^{D} \delta^i(z) \bar{u}^i(x) \tag{1a}$$

$$u_3(x, z) = w(x) + \sum_{i=1}^{D} \delta^i(z) \bar{w}^i(x) \tag{1b}$$

where D is the number of delaminations, u and w are the displacements of a point $(x, 0)$ on the reference surface of the laminate, and u^j are nodal values of displacements in the x direction of each lamina. The terms $\bar{u}^i$ and $\bar{w}^i$ represent possible jumps in the slipping and opening displacements, respectively, at the $L(i)$th delaminated interface. $L(i)$th denotes the location of the interface where the ith delamination lies (Fig. 2), and $\phi^j(z)$ is a linear Lagrangian interpolation function through the thickness of the laminate. The step function $\delta^i(z)$ can be represented as a Heaviside unit step function $H(z)$.

$$\delta^i(z) = H(z - z_{L(i)}) \tag{2}$$

The nonzero components of strain associated with the small displacement theory of elasticity are given by

$$\epsilon_x = \frac{du}{dx} + \sum_{j=1}^{N} \phi^j \frac{du^j}{dx} + \sum_{i=1}^{D} \delta^i \frac{d\bar{u}^i}{dx} \tag{3a}$$

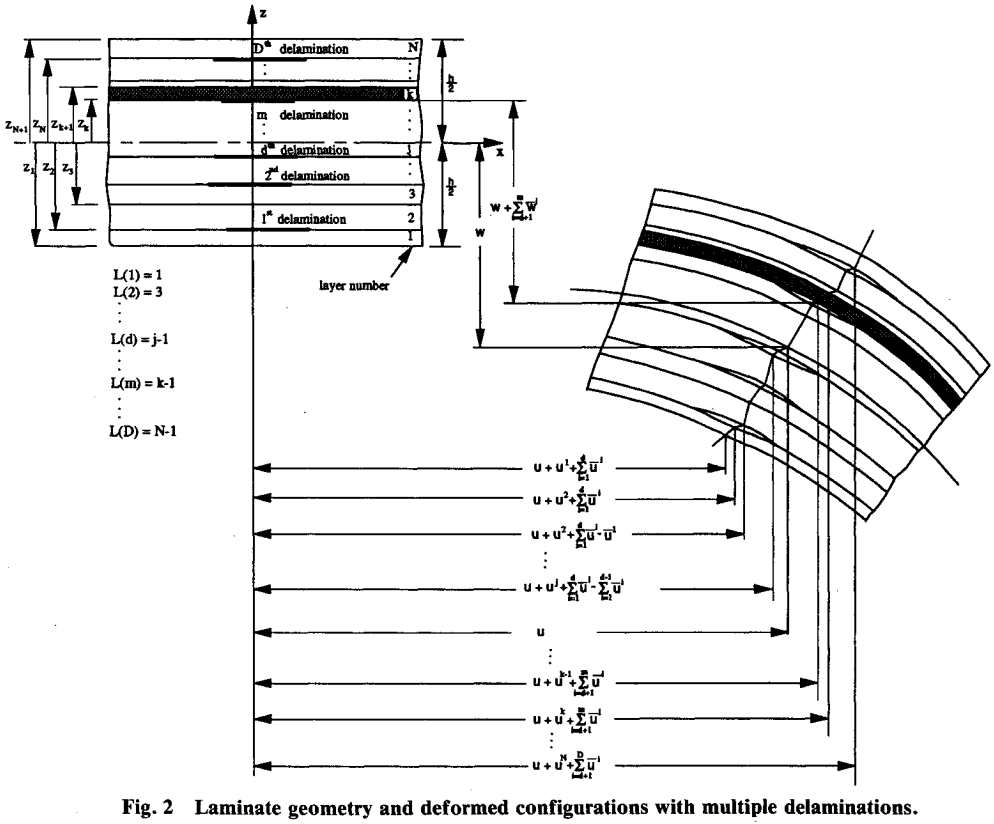

Fig. 2 Laminate geometry and deformed configurations with multiple delaminations.

$$\gamma_{xz} = \frac{dw}{dx} + \sum_{j=1}^{N} \frac{d\phi^j}{dz} u^j + \sum_{i=1}^{D} \delta^i \frac{d\bar{w}^i}{dx} \tag{3b}$$

Equilibrium Equation

The total potential energy of the system can be stated, in its buckled shape, as

$$\Pi = U + V \tag{4}$$

where U is the strain energy

$$U = \frac{1}{2}\int_V \sigma_{ij}\epsilon_{ij}\, dV \tag{5}$$

and V is the potential of the applied loads due to transverse deflection:

$$V = \frac{1}{2}\int_\Omega N_x^o \left(\frac{du_3}{dx}\right)^2 d\Omega \tag{6}$$

Thus, the principle of the stationary value of the total potential energy for the layer-wise theory can be written as

$$0 = \int_V \sigma_{ij}\delta\epsilon_{ij}\, dV + \int_\Omega N_x^o \frac{du_3}{dx}\frac{d\delta u_3}{dx}\, d\Omega \tag{7}$$

Substituting the kinematic relations of Eqs. (1) and (3) into Eq. (7), we obtain the weak statement of the present theory,

$$\begin{aligned} 0 = \int_0^{L/2} \Bigg[& N_x \frac{d\delta u}{dx} + Q_x \frac{d\delta w}{dx} + \sum_{j=1}^{N} \left(N_x^j \frac{d\delta u^j}{dx} + Q_x^j \delta u^j \right) \\ & + \sum_{i=1}^{D} \left(\bar{N}_x^i \frac{d\delta \bar{u}^i}{dx} + \bar{Q}_x^i \frac{d\delta \bar{w}^i}{dx} \right) + N_x^o \frac{dw}{dx}\frac{d\delta w}{dx} \\ & + \sum_{i=1}^{D} \bar{N}_x^{io} \left(\frac{dw}{dx}\frac{d\delta \bar{w}^i}{dx} + \frac{d\delta w}{dx}\frac{d\bar{w}^i}{dx} \right) \\ & + \frac{1}{2}\sum_{i=1}^{D}\sum_{j=1}^{D} \bar{N}_x^{ijo} \left(\frac{d\bar{w}^i}{dx}\frac{d\delta \bar{w}^j}{dx} + \frac{d\delta \bar{w}^i}{dx}\frac{d\bar{w}^j}{dx} \right) \Bigg] dx \end{aligned} \tag{8}$$

where

$$[N_x,\ N_x^j,\ \bar{N}_x^i] = \int_{-h/2}^{h/2} \sigma_x [1,\ \phi^j(z),\ \delta^i(z)]\, dz \tag{9a}$$

$$[Q_x,\ Q_x^j,\ \bar{Q}_x^i] = \int_{-h/2}^{h/2} \tau_{xz} \left[1,\ \frac{d\phi^j}{dz},\ \delta^i(z) \right] dz \tag{9b}$$

In Eq. (8), N_x^o, $\bar{N}_x^{jo}$, $\bar{N}_x^{ijo}$ are the constant in-plane edge loads defined, respectively, by the following:

$$N_x^o = -\lambda n, \qquad \bar{N}_x^{jo} = -\lambda n^j, \qquad \bar{N}_x^{ijo} = -\lambda n^{ij} \tag{10}$$

where λ is a buckling load parameter, n is the specified value of the compressive in-plane force, and n^j and n^{ij} are newly-introduced layer-wise variables given as

$$n^j = \frac{\sum_{k=1}^{N} \int_{Z_k}^{Z_{k+1}} \delta^j\, dz}{\sum_{k=1}^{N} \int_{Z_k}^{Z_{k+1}} dz} n, \qquad n^{ij} = \frac{\sum_{k=1}^{N} \int_{Z_k}^{Z_{k+1}} \delta^i\delta^j\, dz}{\sum_{k=1}^{N} \int_{Z_k}^{Z_{k+1}} dz} n \tag{11}$$

The one-dimensional equilibrium equation of the layer-wise plate theory for buckling analysis can be derived by integrating the derivatives of the varied quantities by parts and collecting the coefficients of δu, δw, δu^j, $\delta \bar{u}^i$, $\delta \bar{w}^i$:

$$\frac{dN_x}{dx} = 0 \tag{12a}$$

$$\frac{dQ_x}{dx} + N_x^o \frac{d^2w}{dx^2} + \sum_{j=1}^{D} \bar{N}_x^{jo} \frac{d^2\bar{w}^j}{dx^2} = 0 \tag{12b}$$

$$\frac{dN_x^j}{dx} - Q_x^j = 0 \tag{12c}$$

$$\frac{d\bar{N}_x^i}{dx} = 0 \tag{12d}$$

$$\frac{d\bar{Q}_x^i}{dx} + \bar{N}_x^{io} \frac{d^2w}{dx^2} + \sum_{j=1}^{D} \bar{N}_x^{ijo} \frac{d^2\bar{w}^j}{dx^2} = 0 \tag{12e}$$

The equilibrium equations consist of $(2 + N + 2D)$ differential equations in $(2 + N + 2D)$ dependent variables (u, w, u^j, $\bar{u}^i$, $\bar{w}^i$). The geometric and forced boundary conditions are on u, w, u^j, $\bar{u}^i$, $\bar{w}^i$, and on N_x, Q_x, N_x^j, $\bar{N}_x^i$, $\bar{Q}_x^i$, where $j = 1, 2, \ldots, N$ and $i = 1, 2, \ldots, D$.

Constitutive Equations

The constitutive equations of the kth orthotropic lamina in the laminate coordinate system are given by

$$\sigma_x^{(k)} = \bar{Q}_x^{(k)} \epsilon_x^{(k)}, \qquad \tau_{xz}^{(k)} = \bar{Q}_{55}^{(k)} \gamma_{xz}^{(k)} \tag{13}$$

where $\bar{Q}_{11}^{(k)}$ and $\bar{Q}_{55}^{(k)}$ denote the transformed stiffnesses of the kth layer.

Substitution of Eq. (13) into Eq. (9) yields the constitutive equations of the laminate

$$N_x = A_{11}\frac{du}{dx} + \sum_{j=1}^{N} B_{11}^j \frac{du^j}{dx} + \sum_{j=1}^{D} E_{11}^i \frac{d\bar{u}^i}{dx} \tag{14a}$$

$$N_x^j = B_{11}^j \frac{du}{dx} + \sum_{k=1}^{N} D_{11}^{jk} \frac{du^k}{dx} + \sum_{i=1}^{D} F_{11}^{ij} \frac{d\bar{u}^i}{dx} \tag{14b}$$

$$\bar{N}_x^i = E_{11}^i \frac{du}{dx} + \sum_{j=1}^{N} F_{11}^{ij} \frac{du^j}{dx} + \sum_{r=1}^{D} E_{11}^{ir} \frac{d\bar{u}^r}{dx} \tag{14c}$$

$$Q_x = A_{55}\frac{dw}{dx} + \sum_{j=1}^{N} B_{55}^j u^j + \sum_{i=1}^{D} E_{55}^i \frac{d\bar{w}^i}{dx} \tag{14d}$$

$$Q_x^j = B_{55}^j \frac{dw}{dx} + \sum_{k=1}^{N} D_{55}^{jk} u^k + \sum_{i=1}^{D} F_{55}^{ij} \frac{d\bar{w}^i}{dx} \tag{14e}$$

$$\bar{Q}_x^i = E_{55}^i \frac{dw}{dx} + \sum_{j=1}^{N} F_{55}^{ij} u^j + \sum_{r=1}^{D} E_{55}^{ir} \frac{d\bar{w}^r}{dx} \tag{14f}$$

where A_{11}, B_{11}^j, etc. are the stiffnesses of the laminate as given in Ref. 18.

Finite Element Model

The generalized displacements (u, w, u^j, $\bar{u}^i$, $\bar{w}^i$) are expressed over each element as a linear combination of the one-dimensional Lagrangian interpolation function ψ_l and the nodal values (u_l, w_l, u_l^j, $\bar{u}_l^i$, $\bar{w}_l^i$)

$$(u,\ w,\ u^j,\ \bar{u}^i,\ \bar{w}^i) = \sum_{l=1}^{n} (u_l,\ w_l,\ u_l^j,\ \bar{u}_l^i,\ \bar{w}_l^i)\psi_l \tag{15}$$

Substituting these expressions into the weak statement of Eq. (8), the finite element model of a typical element is obtained as

$$([K] - \lambda[S])\{\Delta\} = \{0\} \tag{16}$$

where $[K]$, λ, $[S]$, and $\{\Delta\}$ are the stiffness matrix, the eigenvalues, the geometric stiffness matrix, and the eigenvector of nodal displacements corresponding to an eigenvalue, respectively. The explicit forms of $[K]$ and $[S]$ are given in Ref. 18.

Numerical Examples and Discussion

Many previous investigators applied an axial symmetry assumption for composite with symmetric geometry in the axial direction. As a result, antisymmetric modes have been neglected for symmetric geometry problems. In the present study, however, both symmetric and antisymmetric modes are investigated using a half-model of the composite. A typical

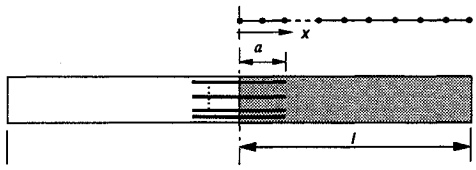

Fig. 3 Typical finite element model for symmetrically located delaminations in the axial direction.

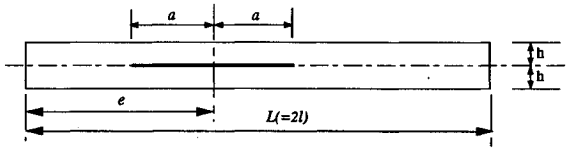

Fig. 4 Geometry for one delamination at midplane.

finite element model is shown in Fig. 3. The following clamped boundary conditions for symmetric and antisymmetric modes are assumed:

At $x = l$:

$$u = 0, \quad w = 0, \quad u^j = 0, \quad \bar{u}^i = 0, \quad \bar{w}^i = 0 \tag{17a}$$

Along $x = a$ to l:

$$\bar{u}^i = 0, \quad \bar{w}^i = 0 \tag{17b}$$

At $x = 0$ for symmetric mode

$$u = 0, \quad u^j = 0, \quad \bar{u}^i = 0 \tag{17c}$$

At $x = 0$ for antisymmetric mode

$$w = 0, \quad \bar{w}^i = 0 \tag{17d}$$

Single Delamination at Midplane

First, a specially orthotropic composite laminate containing one centrally located ($e/L = 0.5$) midplane delamination is considered (Fig. 4) and effects of various geometric parameters on buckling load and buckling mode are studied. The material properties are given as follows: $E_1 = 181$ GPa, $E_2 = 10.3$ GPa, $G_{12} = 7.17$ GPa, $\nu_{12} = 0.28$, where E_1 is Young's modulus in the fiber direction, E_2 is Young's modulus in the transverse direction, G_{12} is the shear modulus, and ν_{12} is the major Poisson's ratio.

The thickness-to-span ratio (h/l) is assumed to be very small (1/400), so results can be compared with solutions from classical lamination theory. Nondimensional buckling loads for three possible buckling modes (Fig. 5) of different delamination length ratio are compared with those from Refs. 2 and 8 in Table 1. Here, the quantity a/l is the ratio of delamination length to beam length. Results obtained by Simitses et al.[2] did not apply symmetry assumptions in the axial direction. On the other hand, symmetry was assumed in Ref. 8, and thus the antisymmetric modes were not considered. The present analysis clearly shows that the nondimensional buckling load for global symmetric and antisymmetric modes correspond to those of Chen and Simitses, respectively, for $a/l = 0.4$, implying that the antisymmetric mode is the first buckling mode for this specific value of a/l. For other values of a/l, the present results for the global symmetric mode are in excellent agreement with the two other solutions.

Nondimensional buckling loads for the three distinguishable buckling modes of a laminate with a single delamination at the midplane are shown in Fig. 6 for two different thickness (h) to span (l) ratio ($h/l = 1/400$ and $1/10$), respectively. In Fig. 6, the filled circles denote the case of $h/l = 1/10$, while the open rectangles denote the case of $h/l = 1/400$. The global symmetric, local symmetric, and antisymmetric modes are presented by solid lines, dashed lines, and dotted lines, respectively. The buckling load N has been normalized with respect to the critical buckling load for the undelaminated composite N_{cr}. It is observed that the global symmetric mode is insensitive to the slenderness ratio of the composite except for large delamination lengths a/l. On the other hand, the local symmetric mode shows a substantial change in load-carrying capacity due to changes in slenderness of the composite. For short delaminations ($a/l < 0.25$), the global symmetric mode is

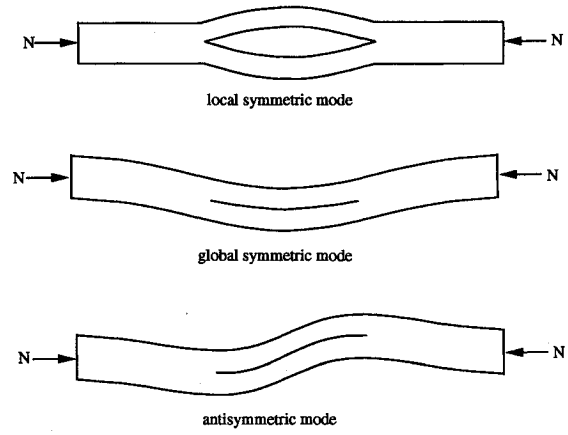

Fig. 5 Buckling mode shapes for one delamination at midplane.

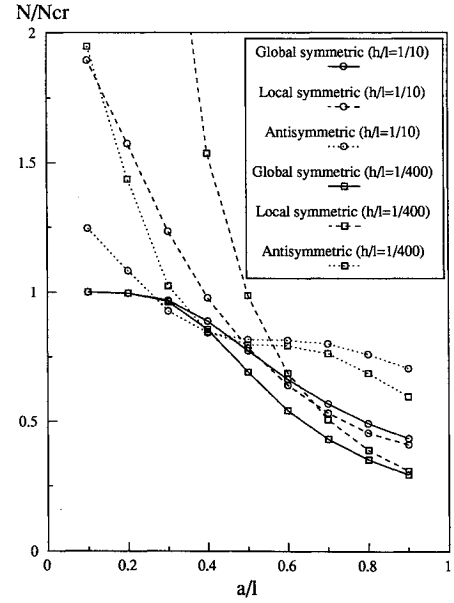

Fig. 6 Nondimensional buckling load vs delamination length for a midplane delamination.

Table 1 Comparison of nondimensional buckling loads for various length of a midplane delamination

			Present		
a/l	Simitses[2]	Chen[8]	Global symmetric	Local symmetric	Anti-symmetric
0.1	0.9999	0.9999	0.9999	15.320	1.9480
0.2	0.9956	0.9956	0.9956	6.0963	1.4360
0.3	0.9638	0.9638	0.9639	2.7176	1.0240
0.4	**0.8481**	**0.8561**	**0.8562**	**1.5358**	**0.8482**
0.5	0.6896	0.6896	0.6898	0.9864	0.7967
0.6	0.5411	0.5411	0.5413	0.6868	0.7929
0.7	0.4310	0.4310	0.4311	0.5058	0.7629
0.8	0.3514	0.3514	0.3515	0.3883	0.6857
0.9	0.2923	0.2933	0.2934	0.3077	0.5947

apparently the first buckling mode for both slenderness ratios. However, between $a/l = 0.25$ and $a/l = 0.45$, the antisymmetric mode becomes the first buckling mode shape for the thick composite, whereas the antisymmetric mode governs the buckling behavior for a very small range of a/l (near 0.4) for the thinner composite. Near $a/l = 0.5$, buckling loads of all three modes are very close to one another, suggesting that the actual failure of a thick composite may be a mixed form of the three modes. For longer delaminations ($a/l > 0.5$), the buckling load of the local symmetric mode is slightly lower than the global symmetric mode for the thick composite, but is still greater than the global symmetric mode of the thinner composite. The antisymmetric mode is far beyond these two modes for both cases, so that failure loads follow either the global or local symmetric buckling mode, depending on the thickness-to-span ratio.

Two and Three Delaminations

For comparison purposes, we examine the problem (Fig. 7) solved by Wang et al.[11] This example demonstrates the effects of nondimensional delamination length (a/l), through-the-thickness location (t/h), and the number of delaminations on the buckling load of laminates. Two cases are considered: two delaminations symmetrically located with respect to the midplane and three delaminations where the additional delamination is at the midplane.

Nondimensional buckling load vs nondimensional delamination length for composites with two and three delaminations

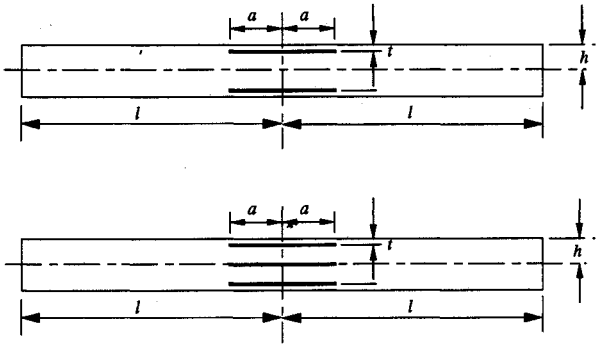

Fig. 7 Two and three symmetrically located delaminations through the thickness.

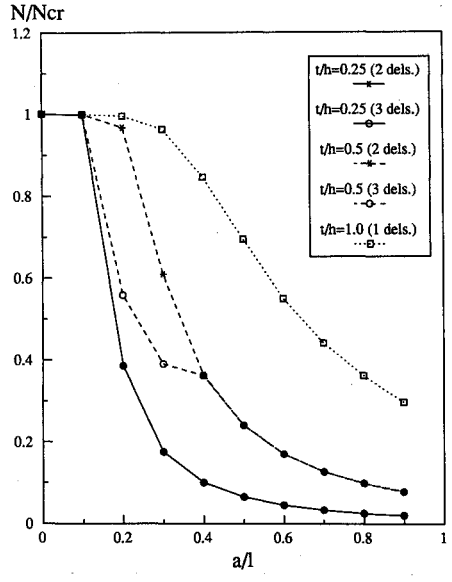

Fig. 8 Nondimensional buckling load vs delamination length for composites containing one, two, and three delaminations with different t/h.

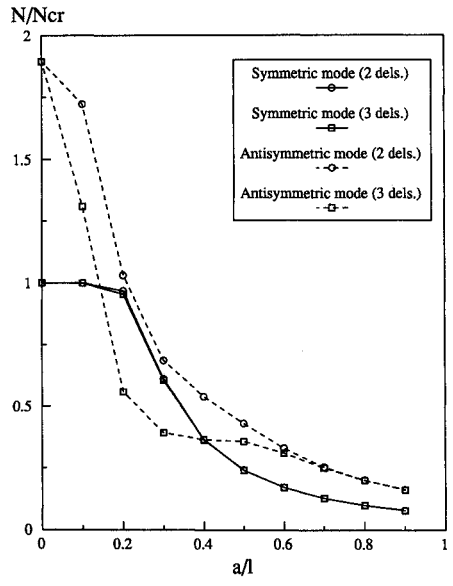

Fig. 9 Nondimensional buckling load vs delamination length for composites containing two and three delaminations with $t/h = 0.5$.

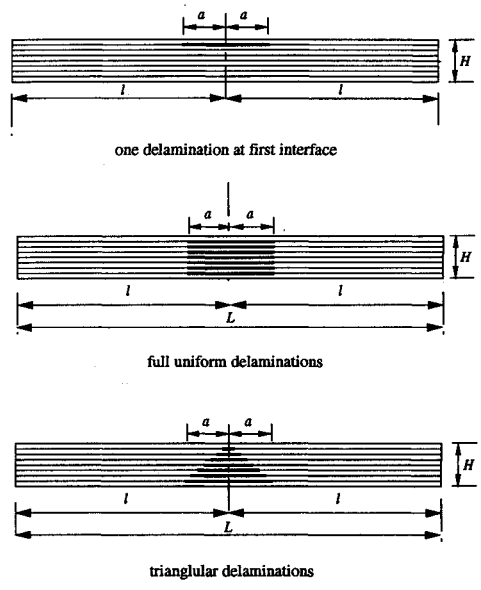

Fig. 10 Various types of delaminations.

is shown in Fig. 8. The results obtained are in good agreement with the results by Wang et al.,[11] except for the case of three delaminations with $t/h = 0.5$. This is because the antisymmetric mode, which is the first buckling mode in this case, was neglected in Ref. 11. To explain this further, the first symmetric and antisymmetric buckling modes for the case of $t/h = 0.5$ are presented in Fig. 9. For the case of $t/h = 0.25$, the outer delaminated regions are much thinner compared to the inner regions for both of the two and three delamination cases. Therefore, the symmetric thin film buckling mode is dominant for both cases and the center delamination stays closed. However, in the case of a composite having $t/h = 0.5$ with three delaminations, the antisymmetric mode governs buckling in the range of $a/l = 0.1$ to 0.4, as shown in Fig. 9. That is, while the additional midplane delamination does not affect the symmetric mode, it has substantial contribution to the antisymmetric mode for relatively short delamination cracks. Consequently, the composite with an additional delamination at the midplane exhibits a much lower critical buckling load than the composite with two delaminations.

It should be noted that the no-penetration condition which precludes physically inadmissible modes was checked for all of

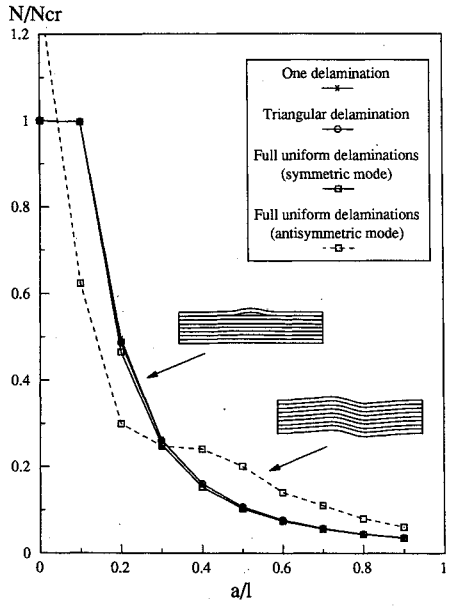

Fig. 11 Nondimensional buckling load vs delamination length for one, triangular, and full uniform delaminations.

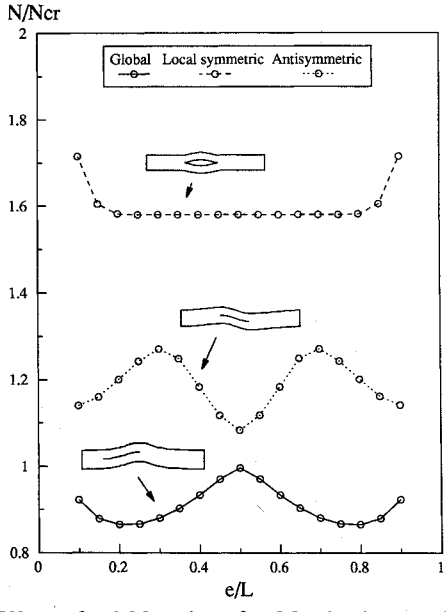

Fig. 12 Effects of axial location of a delamination at midplane for $a/l = 0.2$.

the results presented herein, and none of the critical buckling load results show physically inadmissible buckling modes. The detailed explanation of the no-penetration condition can be found in Lee.[19]

Seven Delaminations

In this case, it is assumed that there are seven interfaces in the laminate where delamination may exist, and each sublaminate has the same thickness. Two different distribution of multiple delaminations are considered (Fig. 10). The thickness-to-span ratio is assumed to be 1/10.

The nondimensional buckling load of the fully delaminated composite with equal delamination lengths is compared in Fig. 11 to a composite containing a single delamination at the outermost interface and a composite with a triangular delamination distribution. It is noted that the single and triangular distribution delamination cases yield almost identical results over the entire region of a/l. That is, the thin-film type local symmetric mode dominates buckling for these two cases. This result suggests that the longest delamination existing in the outermost layer governs the buckling load and mode shape and the shorter ones seldom contribute to the buckling load for the triangular case. However, the buckling load of the fully delaminated composite is far below the other two cases, by 40% for short delamination lengths. This is because the antisymmetric mode, which is insignificant for the other two cases, becomes responsible for buckling of multiple short uniform delaminations. In this case, short delaminations interact with one another, and the composite is severely weakened in its capacity to withstand transverse shear force. It is this susceptibility to shear deformation which accounts for a very low bifurcation load associated with a highly localized antisymmetric mode shape. The global symmetric buckling mode occurs only for very short delaminations, e.g., $a/l < 0.1$ for the one and triangular delaminations, and for $a/l < 0.05$ for full uniform delaminations. For longer delaminations, each sublaminate created by delaminations becomes significantly thin, and thus, thin-film local buckling is predicted, so that the

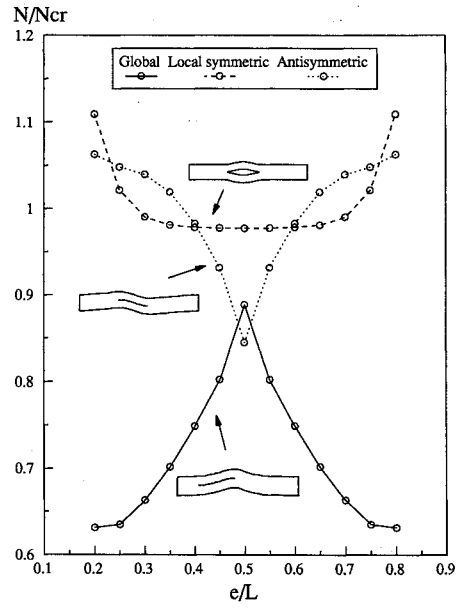

Fig. 13 Effects of axial location of a delamination at midplane for $a/l = 0.4$.

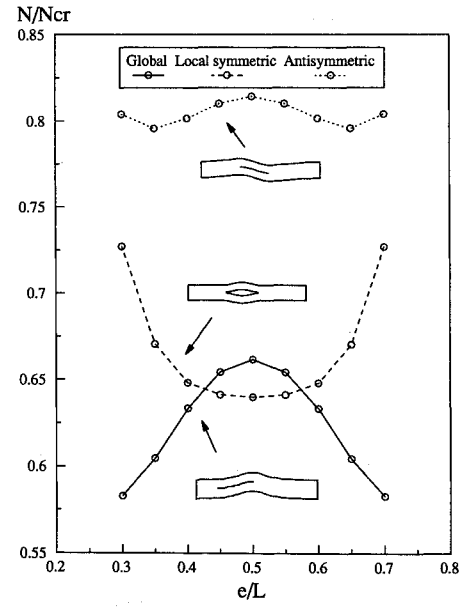

Fig. 14 Effects of axial location of a delamination at midplane for $a/l = 0.6$.

buckling loads for all of the three cases coincide for relatively long delamination cracks ($a/l > 0.3$).

Effect of Axial Location of Delaminations

The effect of delamination location along the axial direction of the composite on the buckling load is shown in Figs. 12–14 for $a/l = 0.2$, 0.4, and 0.6, respectively. The center of the delamination is located at a variable distance e from the left end of the beam (Fig. 4). In Figs. 12–14, three distinguishable buckling modes (global, local symmetric, antisymmetric) are identified.

It is found that the local symmetric mode is increasingly sensitive to axial delamination position as delamination length increases. The buckling load for the local symmetric mode is generally lowest when the delamination lies in the center of the composite, and the buckling load increases as the delamination approaches the support. This is because the effect of the clamped boundary condition becomes significant when the delamination is close to the support. The buckling load for the global mode reaches its highest value when the delamination is located at the midpoint of the composite. The antisymmetric mode also varies with axial delamination location, but it does not exhibit a general tendency for various delamination lengths.

For $a/l = 0.2$, the global mode is dominant for the entire range of e/L. The buckling load is lowest when the delamination is located at the quarter point of the beam. For $a/l = 0.4$, when the delamination is located at the midpoint, the antisymmetric mode is active. Otherwise, the global mode is the first buckling mode. The buckling loads for the local symmetric and antisymmetric modes increase as the delamination approaches the support. For longer delamination ($a/l = 0.6$), the local symmetric mode is the first buckling mode when the delamination is centered near the midpoint of the composite. However, as the delamination becomes off-centered, the buckling load for the local symmetric mode increases due to the clamped boundary condition, and the global buckling mode dominates. The buckling load for the antisymmetric mode is, in this case, far beyond that of the other two buckling modes for the complete range of e/L.

Concluding Remarks

A one-dimensional, layer-wise finite element model was developed to study the compressive stability of composite beam plate with multiple delaminations. The model is capable of predicting accurate buckling loads for various delamination distributions. All of the possible buckling modes including global and local symmetric modes and the antisymmetric mode are considered. The effects of composite geometry and locations, sizes, number, and shapes of delamination on buckling load and mode shape of composite are studied.

Based on the above analytical developments and numerical results, the following conclusions are made:

1) For composites with three delaminations having relatively thin outer sublaminates ($t/h = 0.25$), the additional midplane delamination stays closed and the outer delamination dominates the stability. Thus, the buckling loads and mode shapes are identical to the composite with two delaminations. However, when all of the sublaminates have equal thicknesses ($t/h = 0.5$), the buckling load for the three delamination case becomes much lower than that of the two delamination case in the region where the antisymmetric buckling mode governs the stability of the composite.

2) The thickness-to-span ratio of a delaminated composite affects the buckling load. For a relatively thick composite ($h/l = 1/10$) with a midplane delamination, the three individual buckling modes, e.g., global symmetric, local symmetric, and antisymmetric, govern the buckling behavior of the composite as the delamination length varies. On the other hand, for a thin composite ($h/l = 1/400$), the global symmetric buckling mode is dominant except in the range near $a/l = 0.4$ where the antisymmetric mode governs the buckling mode.

3) The composite with seven uniform delaminations has a much lower buckling load for short delaminations than that for a single delamination at the outermost layer and that of a triangular delamination distribution due to weakened shear strength which results in the antisymmetric mode. It is noted that the larger the number of delaminations, the more dominant is the antisymmetric mode for short uniform delaminations when the delaminations are located symmetrically through the thickness.

4) Axial location of delamination affects buckling load and mode shape significantly. For a given delamination length, the global buckling mode is expected for an off-centered delamination, and the antisymmetric or local symmetric mode is generally expected as a delamination approaches the center of the composite depending on the delamination size.

Acknowledgments

This research work was supported by the Virginia Institute for Material Systems. This support is gratefully acknowledged.

References

[1]Chai, H., Babcock, C. D., and Knauss, W. B., "One-Dimensional Modelling of Failure in Laminated Plates by Delamination Buckling," *International Journal of Solids and Structures,* Vol. 17, No. 11, 1981, pp. 1069–1083.

[2]Simitses, G. J., Sallam, S., and Yin, W. L., "Effect of Delamination of Axially Loaded Homogeneous Laminated Plates," *AIAA Journal,* Vol. 23, No. 9, 1985, pp. 1437–1444.

[3]Sallam, S., and Simitses, G. J., "Delamination Buckling and Growth of Flat, Cross-Ply Laminates," *Composite Structures,* Vol. 4, No. 4, 1985, pp. 361–381.

[4]Yin, W. L., Sallam, S., and Simitses, G. J., "Ultimate Axial Load Capacity of a Delaminated Beam Plate," *AIAA Journal,* Vol. 24, No. 1, 1986, pp. 123–128.

[5]Bottega, W. J., and Maewal, A., "Delamination Buckling and Growth in Laminates," *ASME Journal of Applied Mechanics,* Vol. 50, No. 1, 1983, pp. 184–189.

[6]Sheinman, I., Bass, M., and Ishai, O., "Effect of Delamination on Stability of Laminated Composite Strip," *Composite Structures,* Vol. 11, No. 3, 1989, pp. 227–242.

[7]Kardomateas, G. A., and Schmueser, D. W., "Buckling and Postbuckling of Delaminated Composites Under Compressive Loads Including Transverse Shear Effects," *AIAA Journal,* Vol. 26, No. 3, 1988, pp. 337–343.

[8]Chen, H. P., "Shear Deformation Theory for Compressive Delamination Buckling and Growth," *AIAA Journal,* Vol. 29, No. 5, 1991, pp. 813–819.

[9]Whitcomb, J. D., "Finite Element Analysis of Instability Related Delamination Growth," *Journal of Composite Materials,* Vol. 15, Sept. 1981, pp. 403–426.

[10]Wang, S. S., Zahlan, N. M., and Suemasu, H., "Compressive Stability of Delaminated Random Short-Fiber Composites, Pt. I—Modelling and Methods of Analysis," *Journal of Composite Materials,* Vol. 19, No. 4, 1985, pp. 296–316.

[11]Wang, S. S., Zahlan, N. M., and Suemasu, H., "Compressive Stability of Delaminated Random Short-Fiber Composites, Pt. II—Experimental and Analytical Results," *Journal of Composite Materials,* Vol. 19, No. 4, 1985, pp. 317–333.

[12]Williams, J. F., Stouffer, D. C., Ilic, S., and Jones, R., "An Analysis of Delamination Behavior," *Composite Structures,* Vol. 5, No. 3, 1986, pp. 203–216.

[13]Kapania, R. K., and Wolfe, D. R., "Buckling of Axially Loaded Beam-Plate with Multiple Delaminations," *Advances in Macro-Mechanics of Composite Material Vessels and Components,* edited by D. Hui and T. J. Kojik, PVP Vol. 146, PD Vol. 18, ASME, New York, 1988, pp. 1–10.

[14]Larsson, P. L., "On Multiple Delamination Buckling and Growth in Composite Plates," *International Journal of Solids and Structures,*

Vol. 27, No. 13, 1991, p. 1623–1637.

[15]Kutlu, Z., and Chang, F. K., "Modeling Compression Failure of Laminated Composites Containing Multiple Through-the-Width Delaminations," *Journal of Composite Materials,* Vol. 26, No. 3, 1992, pp. 350–387.

[16]Barbero, E. J., and Reddy, J. N., "Modelling of Delamination in Composite Laminates using a Layer-Wise Plate Theory," *International Journal of Solids and Structures,* Vol. 28, No. 3, 1991, pp. 373–388.

[17]Reddy, J. N., "A Generalization of Two-Dimensional Theories of Laminated Plates," *Communication of Applied Numerical Methods,* Vol. 3, No. 3, 1987, pp. 173–180.

[18]Lee, J., Gurdal, Z., and Griffin, O. H., "A Layer-Wise Approach for the Bifurcation Problem in Laminated Composites with Delaminations," *Proceedings of the AIAA/ASME/ASCE/AHS/ASC 33rd Structures, Structural Dynamics, and Materials Conference* (Dallas, TX), April 1992, pp. 10–20.

[19]Lee, J., "Vibration, Buckling and Postbuckling of Laminated Composites with Delaminations," Ph.D. Dissertation, Virginia Polytechnic Inst. and State Univ., Blacksburg, VA, 1992.